



ELSEVIER

Contents lists available at ScienceDirect

Opto-Electronics Review

journal homepage: <http://www.journals.elsevier.com/opto-electronics-review>

Full Length Article

Light-stimulated electro-optics by azo-doped aerosil/7CB nanocomposites

Georgi B. Hadjichristov^{a,*}, Yordan G. Marinov^b, Alexander G. Petrov^b, Subbarao Krishna Prasad^c^a Laboratory of Optics & Spectroscopy, Georgi Nadjakov Institute of Solid State Physics, Bulgarian Academy of Sciences, 72 Tzarigradsko Chaussee Blvd., Sofia, BG-1784, Bulgaria^b Laboratory of Biomolecular Layers, Georgi Nadjakov Institute of Solid State Physics, Bulgarian Academy of Sciences, 72 Tzarigradsko Chaussee Blvd., Sofia, BG-1784, Bulgaria^c Centre for Nano and Soft Matter Sciences, P.O. Box 1329, Jalahalli, Bengaluru 560 013, India

ARTICLE INFO

Article history:

Received 11 October 2017

Received in revised form 12 March 2018

Accepted 15 April 2018

Available online 26 May 2018

Keywords:

Azo-doped nematic nanocomposites

Silica nanoparticles

Optical films

Electro-optical properties

Photo-controllable electro-optics

ABSTRACT

Photoactive nanofilled nematic is proposed. Stable three-component photoresponsive nanocomposite was prepared from photo-insensitive nanofilled nematic by inclusion of 3 wt.% azobenzene-containing photoactive mesogen 4-(4'-ethoxyphenylazo)phenyl hexanoate (EPH). The host nanofilled nematic was produced from the room-temperature nematic liquid crystal 4-*n*-heptyl cyanobiphenyl (7CB) and 3 wt.% filler of Aerosil 300 hydrophilic silica nanospheres of size 7 nm. Apparent effect of stimulation with a relatively weak continuous illumination by UV light (375 nm wavelength) takes place for both the alternating-current electric field-dependent optical transmittance and the electro-optic amplitude-frequency modulation by thin films (25 μm thick) of the EPH/aerosil/7CB nanocomposite. The light-stimulated electro-optics of EPH-doped aerosil/7CB films and the corresponding reversible light control are achieved through *trans-cis-trans* photoisomerization of the photoactive agent EPH. As such, the initial electro-optical response of the studied photoactive nanocomposites is recovered with continuous blue-light illumination. The examined EPH/aerosil/7CB nanocomposites exhibit photo-controllable electro-optical response that is of practical interest.

© 2018 Association of Polish Electrical Engineers (SEP). Published by Elsevier B.V. All rights reserved.

1. Introduction

The composites of nanoparticles doped liquid crystals (LCs) are not only interesting from fundamental science point of view but also promising for a wide variety of applications in the electronic device industry and technology, as well as in bio-medical research and diagnostics [1–4]. An important advantage of the LC nanocomposites is their relatively easy preparation. Among the challenging types of nanocomposites, LCs doped with silica (SiO₂) nanoparticles attract significant research attention due to their valuable properties and multi-functional applications based on electro-optical (EO) and dielectric response [5–8]. Furthermore, such advanced nanofilled materials are currently of increasing interest driven by the possibility of implementing new EO mechanisms for active control, manipulation and modulation of light. In particular, nanocomposites of aerosil nanoparticles (ANPs) of a size 7–10 nm dispersed in cyano-biphenyl nematic LCs have been widely explored in view of their potential electric and EO applications [9–12]. Using LC-silica dispersions, LC electric lens and scattering-type bistable and multistable LC display devices have been demonstrated [13–15]. Very recently, we have

investigated the EO response of thin (25 μm) films of nanocomposites consisting of room-temperature nematic heptylcyanobiphenyl (abbreviated name 7CB) and 3 wt.% ANPs [16,17]. For the scatter-based electro-optics of ANPs/7CB films we have shown: (i) the possibility to control the optical transmittance and the amplitude of the second harmonic EO modulation by means of the applied alternating-current (AC) voltage, and (ii) that at high AC voltage the second-harmonic EO modulation by such films is almost frequency independent over a wide frequency range.

The fabrication of photoresponsive nanocomposite materials is an advanced trend, e.g., for practical use in organic light-controllable EO devices. For purpose, the nanocomposites may be doped with efficient photoactive compounds, such as azobenzenes whose effective light-induced *trans-cis* conversion can be exploited. It is well known that some azobenzene-doped nematics exhibit a considerable photoactivity [18–21]. Like various novel azobenzene-containing LCs [22,23] and polymers [22,24], as well as other advanced photoresponsive LC systems [25], the azo-doped nanofilled nematics would be useful for widespread practical applications, e.g., for adaptive and photo-controllable electro-optics and photonics. In this context, an effect of ultra-violet (UV) light-induced transparency enhancement upon applying AC electric field was briefly reported for thin films of ANPs/7CB doped with photoactive azobenzene LC compound 4-(4'-ethoxyphenylazo) phenyl hexanoate (EPH for short), and having polyimide alignment layers

* Corresponding author.

E-mail address: georgibh@issp.bas.bg (G.B. Hadjichristov).

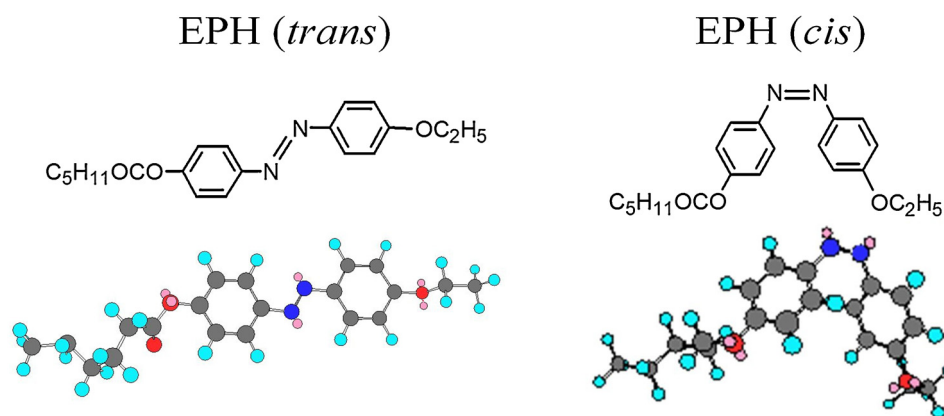


Fig. 1. Diagram depicting the *trans* and *cis* molecular conformers of the azobenzene LC compound EPH.

[26,27]. This effect useful for light control and modulation through the *trans-cis* photoisomerization of the EPH molecules [20] was analyzed as depending on the concentration of the azo nanodopants in ANPs/7CB [28]. Here, we present an expanded experimental study on 25 μm -thick ANPs/7CB films (with 3 wt.% hydrophilic ANPs – Aerosil 300 of size ca. 7 nm) doped with 3 wt.% EPH, aimed to inspect in more details such photo-sensitized nematic nanocomposite structures in view of their feasibility for light-controllable EO applications based on the efficient *trans-cis* photoisomerization upon illumination with continuous light sources.

2. Materials and methods

2.1. Nanocomposite preparation

For the experiments performed, the commercial (from Merck) LC 4'-heptyl-4-biphenylcarbonitrile (abbreviated as 7CB) acted as the host compound. This thermotropic LC has a stable nematic phase at room temperature. Its isotropic-to-nematic phase transition temperature (the clearing point, T_{I-N}) was measured to be 42.35 $^{\circ}\text{C}$ [29]. 7CB exhibits a large positive dielectric anisotropy ($\Delta\epsilon \sim 10$ at frequency 1 kHz and temperature of 25 $^{\circ}\text{C}$ [30]).

As a photoactive agent incorporated in the photo-insensitive 7CB-based nanofilled nematic, we employed 4-(4'-ethoxy phenylazo)phenyl hexanoate (abbreviated hereafter as EPH) procured from Eastman Organics. The chemical structure of EPH is given in Fig. 1. This chemically-, photo- and thermo-stable azo-containing liquid-crystalline compound also exhibits a nematic mesophase at room temperature. The latter feature helps in arriving at homogeneous mixtures of EPH and 7CB. As shown in our previous work [20,21], the inclusion of EPH even at a concentration of 1 wt.% in photo-insensitive nematics makes them photoactive with a potential for device applications. For the present studies, we have used 3 wt.% of EPH in aerosil/7CB nanofilled nematic.

To realize the restricted geometry, hydrophilic aerosil nanoparticles (ANPs) - Aerosil A-300 nanospheres with a mean diameter of ~ 7 nm were used [29]. The ANPs were capped with silanol groups. The preparation of mixtures is described in [29]. The ANPs were mixed with 7CB at concentration of 3 wt.%. At this concentration, nanofilled alkyl/alkoxy cyanobiphenyls (such as 7CB) do form soft gels exhibiting thixotropic properties [31,32].

2.2. Methods and instruments

The samples (plane-parallel thin films with a thickness of 25 μm) were prepared as sandwiched between a pair of 0.7 mm-thick flat glass plates (from Delta Technologies Ltd., USA) separated

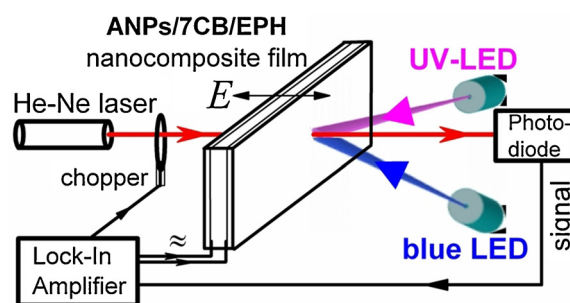


Fig. 2. Schematic drawing of the experimental set-up.

with spacers. The inner surfaces of the glass plates were coated with ~ 80 nm-thick transparent conductive layers of indium tin oxide (ITO) to serve as electrodes with a low ($< 10 \Omega/\text{sq}$) sheet resistance. Further, the ITO surfaces were overcoated with polyimide PI-2555 (from HD Microsystems, USA) and rubbed unidirectional. Owing to the high viscosity of the aerosil composites, the usual method of filling the sample by capillary action was not adopted. Instead, the sample was placed on one substrate and then the second substrate was kept on top and the cell sealed using UV-light-curing epoxy. Caution was taken not to expose the sample area to UV light during this curing process. In this way, films of ANPs/7CB/EPH dispersion were prepared, as well as nanocomposite films of undoped ANPs/7CB gel for comparative measurements. The latter samples were sandwiched by use of identical glass plates (0.7 mm-thick, with ITO & PI-2555 unidirectionally rubbed). In order to assess the net effect from the azo-dopant EPH, complementary measurements of the optical absorption in the UV-vis spectral range were conducted by 25 μm -thick ANPs/7CB/EPH films in cells with quartz plates. The morphology of the nanocomposite films was examined in transmission by means of Zeiss NU-2 polarizing microscope, and imaged using a microscope photcamera (Moticam 2500) interfaced to computer.

For EO measurements, we used a setup (schematically shown in Fig. 2) designed in our laboratory. The EO response of the nanocomposite films was investigated by means of He-Ne laser beam polarized circularly (~ 1 mW optical power, wavelength $\lambda = 632.8$ nm). The laser beam was directed at normal incidence to the sample, the beam diameter on the sample was about 1 mm. The alternating current (AC) electric field was applied perpendicular to the plane of the nanocomposite films, thus coinciding with the direction of the laser beam. The electro-optics of the nanocomposite films, in terms of light transmittance and frequency modulation EO characteristics, were measured by a silicon photodiode in conjunction with a lock-in amplifier (SR830 DSP) controlled

by computer. The output sinusoidal AC voltage was subsequently amplified using a high voltage amplifier (Pintek HA-400) in order to be in the range 0–100 V_{RMS} when applied to the samples.

The photodiode detector was placed at a distance of 30 cm from the sample. By measurements of the static EO characteristics of the films (their optical transmittance as a function of the applied AC voltage at a fixed frequency), the time interval between the data points was 8 s. The frequency spectra of the second harmonic of the transmitted modulated laser beam (dynamic characteristics of the films) were recorded by sweeping the electric field frequency in the range 1 Hz–3 kHz. The photoresponsive ANPs/7CB/EPH nanocomposite films were photo-activated with unpolarized light from two continuous-light LEDs (light-emitting diodes) with stabilized intensity: 'UV-LED' (NSHU550A, Nichia Corporation, Japan) and 'blue LED' (Optica Laser curing unit, model 405-8B), both of a relatively low optical power but with highly directed and uniform outputs. The LEDs were supplied by 4-channel Programmable Linear DC Power Supply Instek GPD-4303S (DC voltage stability $\pm 0.01\%$). The same device was employed to programmable switching of the LEDs in time. The light intensity on the samples were 1.8 mW cm⁻² ($\pm 5\%$) and 5.7 mW cm⁻² ($\pm 3\%$), for the illumination by the UV-LED (peak wavelength of 375 nm) and blue LED (peak wavelength of 455 nm), respectively. At these intensity levels (kept on throughout the measurements), no photo-induced irreversible changes (e.g., photo-chemical) or phase transitions (e.g., surface melting [33]) were observed for the films during our experiments. To reject any reflected or scattered light (UV or blue) from the samples, both the photodiode and the microscope photocamera were equipped with red spectral filter. All experiments were carried out in the dark in order to avoid any influence of other light sources.

The spectra of optical transmittance of the samples were recorded in the wavelength range from 300 nm to 900 nm (spectral resolution of 0.5 nm) using Perkin Elmer Lambda 1050 spectrophotometer. The time response of the films upon illumination with the LEDs was measured with photodiode and analog-to-digital converter (ADC) interfaced to computer (temporal resolution of 1 s). The temperature of the sample was maintained (± 0.1 °C) with hot stage (Mettler FP82 and the associated controller). For the variable-temperature thermo-optical measurements, the light transmittance data were collected (by means of He-Ne laser beam, photodiode and ADC) while the samples were cooled from 39 °C to 26 °C at a rate of 1 °C min⁻¹.

3. Results and discussion

3.1. Optical spectroscopy data

As a rapid means of providing information at molecular level, the optical spectroscopy can be used to look for the changes of the host 7CB nematic upon mixing with ANPs and EPH molecules. Fig. 3 reports the UV–vis light transmittance spectrum of 25 μm -thick ANPs/7CB nanocomposite film as compared to the transmittance of a 25 μm -thick layer of pure 7CB nematic, both in identical cells (from 0.7 mm-thick glass plates with ITO and unidirectionally rubbed polyimide PI-2555 coatings). The modification of the film transmittance due to the dispersed ANPs can be clearly seen. Unfortunately, the plates of the cells we have used exhibited a peculiar transparency (shown also in Fig. 3) which does not allow to unambiguously register and distinguish the spectral subbands specific for the prepared ANPs/7CB/EPH composites (because the cell plates mask the characteristic bands of EPH azobenzene LC admixture that is in relative small amount in ANPs/7CB/EPH).

In order to get a clear spectral evidence for the azo dopants, we recorded the UV–vis absorption of the studied three-component

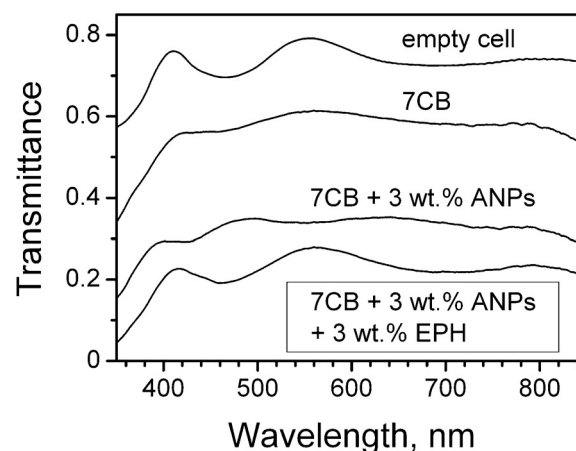


Fig. 3. UV–vis light transmittance spectra recorded for ANPs/7CB/EPH and ANPs/7CB nanocomposites, as well as for pure liquid crystal 7CB, in identical cells (assembled from 0.7 mm-thick glass plates with ITO overcoated with rubbed polyimide). The transmittance spectrum of the same cell with a gap of 25 μm , but empty, is given for reference. The spectra were obtained under identical experimental conditions; temperature 26 °C.

ANPs/7CB/EPH films when they were in cells assembled from quartz plates (without any coatings, neither ITO nor polyimide), also in order to surmount the 50% light cut-off of the optical glass at ~ 380 nm. Thus, the presence of EPH azo-bonded molecules is proven by the spectral band of EPH *trans*-conformers, in our case the broad shoulder at around 370 nm (Fig. 4a) (as known, the *trans*-azobenzenes π – π^* absorption band is close to this wavelength). Further, the absorption spectrum of EPH-doped ANPs/7CB shown in Fig. 4(a) indicates that one can expect an efficient photoactivation of this composite by photoisomerization of the EPH photoactive component by using a light at wavelength of 375 nm that is close to the absorption peak of EPH. The absorption spectrum of EPH oneself is also shown in Fig. 4(a). Actually, the latter spectrum is relevant to a mix of *trans* and *cis* molecular conformers of EPH. By that, the *trans*-state is predominant because this is thermodynamically more stable state (energetically more stable configuration).

For the sake of completeness, Fig. 4(b) represents the photo-induced UV–vis absorption changes related to the *trans*–*cis* conformational changes of the used azobenzene LC EPH, being in concentration of 3 wt.% in the composite material ANPs/7CB/EPH under study. The photo-induced spectral modifications were registered after illumination with either with blue light (to display the absorption of the *trans*-conformers of EPH), or with UV light (to display the absorption of the *cis*-conformers). By these measurements, care was taken to avoid any impact of ambient light (e.g., from luminescent lamps, sunlight, etc.). The recorded spectra reveal two absorption bands centered at ~ 370 nm and ~ 450 nm. They are attributed to π – π^* transition band of the EPH *trans*-isomer and n – π^* transition band of the EPH *cis*-isomer, respectively. As seen from Fig. 4(b), the absorbance of the EPH (*trans*) diminishes by UV light, and in the same time the corresponding absorbance of the EPH (*cis*) increases, clearly indicating the efficient UV-light-induced *trans*–*cis* isomerization of azobenzene contained in the film. Regarding the presence of both kinds of EPH isomers, these spectra reveal two photo-induced states with: (i) large amount of the EPH *trans*-isomers (and low amount of *cis*-isomers) produced with a blue light; and (ii) UV light-activated state with more *cis*-conformed EPH than *trans*-isomers. The relative percentage of both photo-induced EPH isomers in these 'mostly *trans*' and the '*cis*-rich' states, as well as the conversion rate, depend on the intensity/dose of the input light.

At the wavelength range of the emission of the UV-LED we have employed, 7CB in the nematic state exhibits practically no absorp-

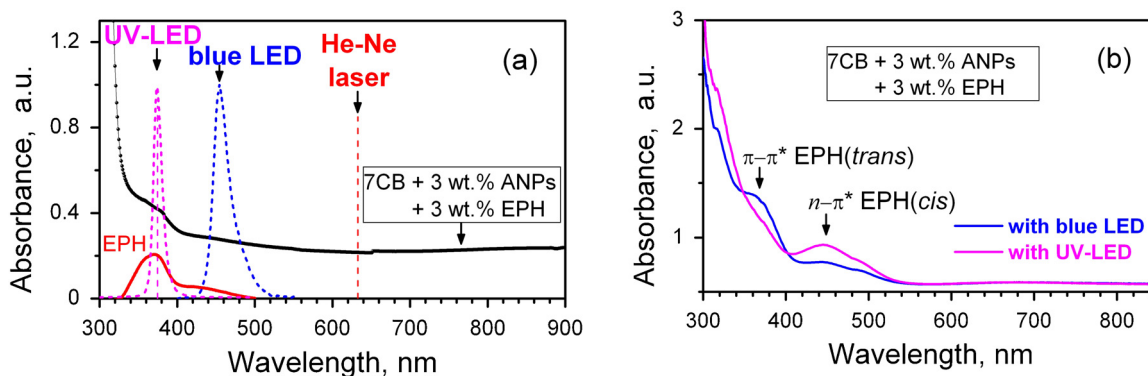


Fig. 4. (a) UV–vis absorption spectrum of 25 μm -thick ANPs/7CB/EPH nanocomposite film between quartz plates. For comparison, the spectrum of solution of EPH (1 wt.%) in transparent organic solvent (measured in a quartz cuvette with optical path of 1 mm) is also shown (down). The emission spectra of the UV-LED and the blue LED employed, are also plotted (dashed), as well as the position of He-Ne laser wavelength. (b) UV–vis absorption spectra of 25 μm -thick ANPs/7CB/EPH film in a cell assembled from 0.7 mm-thick glass plates with ITO overcoated with rubbed polyimide. The spectra were recorded at 24 $^{\circ}\text{C}$ after illumination either with blue LED for 3 min., or with UV-LED for 3 min.

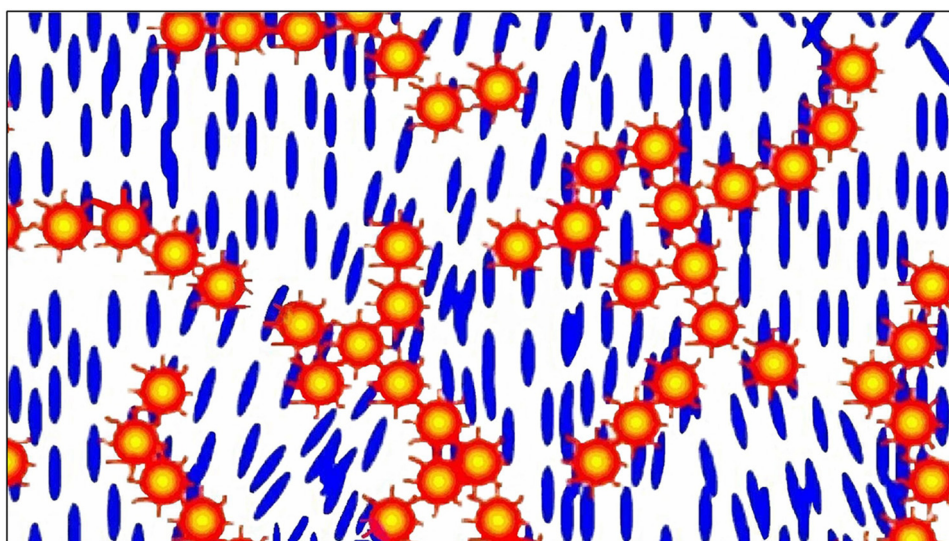


Fig. 5. Illustration of the structure of nano(aerosil)-filled nematic. The gel network is formed by ANPs (colored in orange); the hydrophilic aerosil "coronas" from silanol groups decorating the aerosil nanospheres are also depicted. The liquid-crystal molecules, in our case nematic 7CB, are colored with blue.

tion (according to data, obtained either by optical spectroscopy, for instance [34], or by ultra-performance convergence chromatography [35]). The significant absorption of 7CB is below 320 nm. On the other hand, the fact that 7CB contains no triple bond or double bond, makes this LC compound quite resistant to UV exposure (in fact, no sign of any photo-degradation was observed in the course of our experiments). Incidentally, 7CB also does not exhibit significant absorption in the blue (430 nm–500 nm) and in the red (633 nm) wavelength regions (see Fig. 4a). In contrast, one should note the strong absorption of EPH-doped ANPs/7CB films in the visible, resulting in their yellow color, as well as the strong light scattering by these films (at zero field, no voltage applied) in the whole spectral range considered here (namely as a result of light scattering, the baseline of the spectrum of ANPs/7CB/EPH film in Fig. 4(a) is in a high position). The wavelength of He-Ne laser ($\lambda = 633 \text{ nm}$) is very suitable for measurements of the electro-optical response of our ANPs/7CB/EPH nanocomposite films. Also taking into account the appropriate transmittance of the cell plates ($\sim 80\%$) at this wavelength. Actually, any laser source with a visible wavelength above 600 nm is proper. As seen from Fig. 4(a), such a wavelength is beyond the spectral range of the strong absorbance of EPH and its photoactivity. Furthermore, at minimum absorbance of the studied ANPs/7CB/EPH films (Fig. 4a) one can

avoid any undesirable effects leading to their heating and photo-degradation.

Just as in ANPs/7CB, the strong light scattering by the ANPs/7CB/EPH films does result from the structure formed in this kind of nematic nanocomposites (namely a soft gel, weak gel) [11,29,31,32]. Such filled nematic dispersions exhibit inhomogeneous morphology due to ANPs agglomerates [36,37] of macroscopic and submicron sizes, as well as some local variations of concentration due to agglomerate segregation. As known, the large-scale structure of the aggregates is responsible for the intensity at small scattering angles, and the small-scale structure of the aggregates determines the intensity at large scattering angles (the contributions of the various sizes of the aggregates can be hardly resolved).

In more details, an irregular and fragile gel network is formed in nano(aerosil)-filled nematics, like ANPs/7CB nanocomposite [12] (Fig. 5) that exhibits a spatial confinement. This hydrogen bond network of ANPs is caused by the interactions between the silanol groups decorating the aerosil nanospheres and renders the quenched random disorder to be created *in situ*. The feature that the confined geometry in filled nematics [7,9,13] introduces a disorder is well established for these heterogeneous nanostructured LC systems [38–41], in particular, for ANPs/7CB dispersions hav-

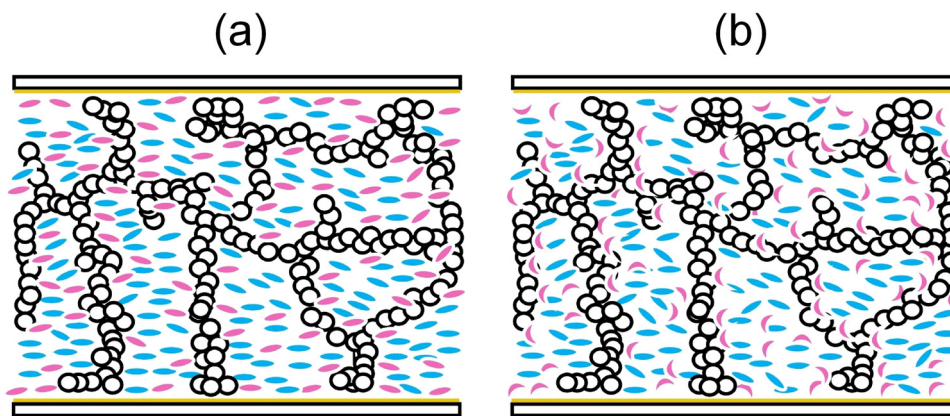


Fig. 6. Sketch of morphology of the studied nanocomposite film of ANPs/7CB/EPH in its nematic state. The film is in a cell with polyimide orienting layers (colored in yellow in the picture) over ITO glass plates. No electric field applied. The gel network formed by ANPs is drawn by circles, the molecules of the nematic 7CB are depicted colored in blue. The LC molecules of the EPH azo dopants are presented colored in violet: (a) *trans*-conformed; (b) *cis*-conformed.

ing concentration and size of ANPs as the presently studied [29]. Indeed, such dispersion of ANPs in the nematic 7CB destabilizes the nematic ordering of the host 7CB and reduces T_{I-N} from 42.35 °C to 41.9 °C [29].

The LC material in ANPs/7CB gel does scatter light namely by local inhomogeneities due to the ANPs dopants, and the scattering can be electrically-controllable (in simple terms, the ANPs generate orientation defects in anisotropic liquid-crystalline matrix, and the orientation of the molecules of the nematic 7CB in electric field leads to a diminishing the effect of these defects). To a large extent, the EO performance of the examined nanocomposites is determined from the agglomeration and segregation of ANPs dispersed in the nematic LC, *i.e.* the performance of this nano-structured material is directly related to the concentration of ANPs.

Clearly, the EPH admixture in the ANPs/7CB nanocomposite introduces an additional disorder in the bulk of the three-component mixed system ANPs/7CB/EPH. As for the orientation of the EPH molecules within this system in its nematic state, the EPH *trans*-conformers are expected to be directed mostly tangentially toward the 7CB molecules (Fig. 6a). The orienting polyimide layers over the ITO glasses of the cells used for our experiments will promote a planar orientation of the LC molecules in the nematic phase (such alignment should be well pronounced close to the orienting layers). However, inside the film the LC molecules become less aligned due to the presence of ANPs chains. Since both peripheral sides of the EPH molecule consist of hydrophobic tails, in vicinity of the long and randomly crossing ANPs chains these molecules are not tagged to the hydrophilic ANPs. In the bulk of the gel film (Fig. 6b), the randomly distributed *cis*-conformers efficiently enhance the disorder of the nematic gel system because of the lower anisotropy of the *cis*-state.

Fig. 7 presents the light transmittance of ANPs/7CB/EPH film versus the temperature. As seen, T_{I-N} of EPH-doped ANPs/7CB nanocomposite is significantly lower than that of undoped ANPs/7CB (~ 42 °C [29]). When the EPH molecules are in their *trans*-forms, $T_{I-N}^{noUV} = 37$ °C. More importantly, upon UV light a relatively large lowering (of about 7 °C) of T_{I-N} is evident. This isomerization-induced feature is well known (photo-driven phase transformation, photo-induced isotropic phase, an isothermal transition from the nematic to isotropic). Unlike the rod-like *trans*-form that is compatible with the formation of the LC phase, the bent *cis*-form will destabilize the LC phase, and thus one can expect that the *trans*-to-*cis* conformation generally reduces T_{I-N} [18] (*i.e.*, $T_{I-N}^{UV} < T_{I-N}^{noUV}$). In fact, with UV light at comparable intensity (~ 1 mW cm⁻²) similar shift of T_{I-N} was reported for polyimide oriented planar films of a guest-host mixture of 3.4 wt.% EPH in 7CB [42].

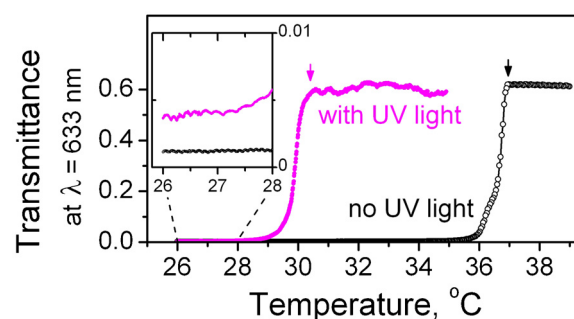


Fig. 7. The thermal variation of light transmittance of ANPs/7CB/EPH film in the cooling mode without applying an electric field. The film was initially illuminated with a blue light and then measured (open circles) and subsequently UV-light illuminated (the blue light turned off) and so measured (solid circles). The arrows indicate the transition temperatures. The inset shows the same data on an expanded scale (from 26 °C to 28 °C in the temperature range of the nematic phase).

3.2. Alteration of the EO response of ANPs/7CB/EPH nanocomposite by light

3.2.1. Film morphology and AC field-dependent transmittance

Fig. 8 shows optical microscope images of ANPs/7CB/EPH film texture (the temperature of the film was kept a few degrees below T_{I-N}^{UV}). Micrometer-scaled regions of disordered textural formations of LC material containing agglomerates of ANPs were present. The UV-light induced changes were well observable at higher voltage of the AC electric field applied on the sample. Both photo-induced and the electrically-driven EO effect appear like a brightening of the texture – the ANPs/7CB/EPH nanocomposite films are cleared up. After the removal of the UV light, the samples retain this state for enough time, *e.g.* for hours (notice, this holds at the UV light intensity employed here, as well as at the present concentrations of EPH and ANPs, each of 3 wt.%). During this time takes place a very slow gradual return to the initial state of the sample (*i.e.*, the state before the exposure upon UV light) in which the EPH molecules are mostly in their *trans*-forms. Such *cis*-to-*trans* transformation of the EPH molecular shape occurs spontaneous in the “dark” (and in the absence of electric field) by the process of thermal back relaxation.

Similarly to undoped ANPs/7CB nanocomposite [16,17,29], the voltage-induced increase of the transparency of ANPs/7CB/EPH films seen in Fig. 8 is because of the AC electric-field-driven reorientation of the LC molecules along the electric field direction, from the surface dictated planar to the homeotropic orientation induced by higher magnitude of the applied electric field (and due to the posi-

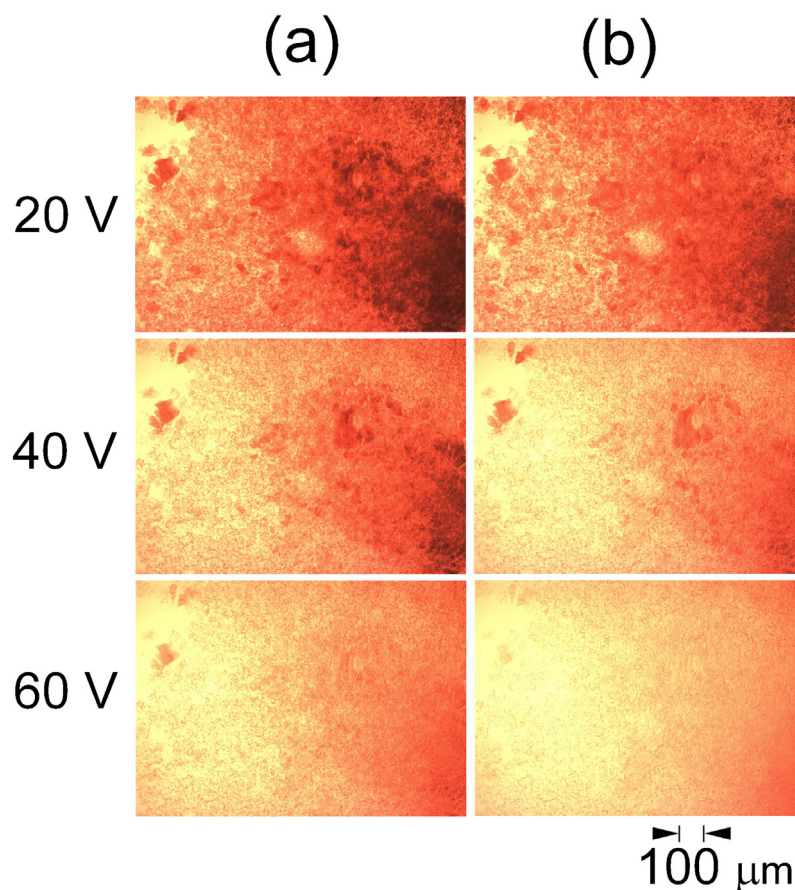


Fig. 8. Micrographs taken after illumination of ANPs/7CB/EPH film with: (a) blue light; (b) UV light. AC (1 kHz) voltages applied on the film: 20 V_{RMS} ; 40 V_{RMS} and 60 V_{RMS} . The other experimental conditions were kept the same, and the temperature of the film was maintained at 26 °C.

tive dielectric anisotropy of all the components – 7CB, EPH, EPH/7CB mixture [42] as well as of the composite material ANPs/7CB/EPH as a whole). On the other hand, the photo-induced EO effect results from UV-light induced photoisomerization of azobenzene EPH (the transformation from elongated rod-like *trans* isomers to bent *cis* isomers, recall Fig. 1) [18–21] within the illuminated area of the films. Reasonably, no such distinct photo-induced textural changes were observed for undoped ANPs/7CB films in identical cells and under the same experimental conditions.

We have to point out that the morphology images of the studied nanocomposite films did not depend on the polarization of the incoming light, a feature also true for their EO characteristics discussed below. This is owing to the lack of planar orientation of the films despite the unidirectional rubbing of the inner surface of the cell plates. Obviously, the absence of LC molecular alignment (as proved by polarizing microscope) does result from the strong random disorder of the studied nematic gel structure due to the ANPs fillers [16]. That is why, no polarizers were used by the experiments described below.

Understandably, the electrically- and UV-light induced morphology change of ANPs/7CB/EPH films does reflect in their light transmittance characteristics. Fig. 9(a) presents the He-Ne laser beam transmission through ANPs/7CB/EPH nematic film versus the applied AC voltage, after an illumination with blue light or UV light at 375 nm. According to the well established mechanism of light scattering by nanofilled nematics [13,38], the electrically-driven reorientation of LC molecules having positive dielectric anisotropy leads to reduction of scattered light with increasing AC electric field and thereby to increase of film transparency. Thus, an electrical control of the film transparency can be readily achieved.

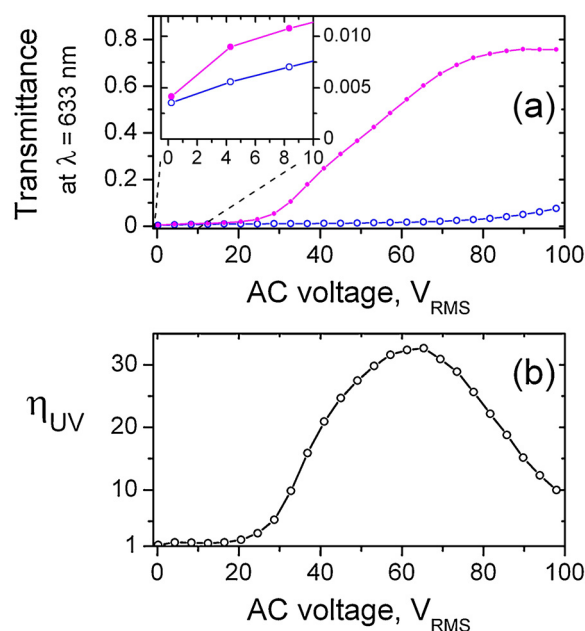


Fig. 9. (a) Electric-field-dependent light transmittance of ANPs/7CB/EPH nematic film after illumination with: (a) blue-light (circles); UV light (points). The frequency of the applied electric field was 1 kHz. The temperature of the film was maintained at 26 °C. The inset presents the low-voltage region of the same plots on an expanded scale; (b) the degree (η_{UV}) of the UV-light induced effect for the ANPs/7CB/EPH film (the ratio of the with/without datasets in (a) as a function of the applied AC voltage.

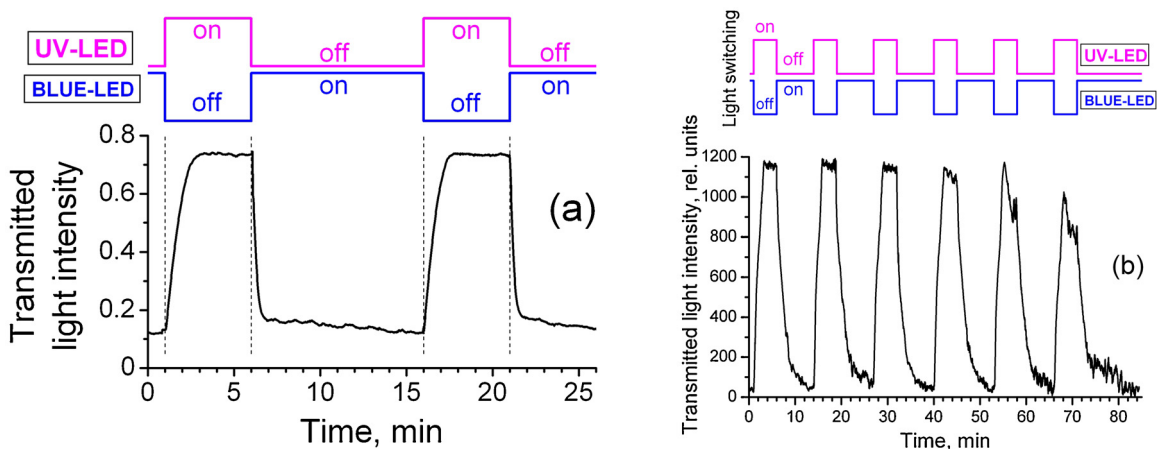


Fig. 10. Photo-switching of the electro-optics of ANPs/7CB/EPH nanocomposite film (temporal response) probed by He-Ne laser beam. The film was illuminated by UV-LED and alternatively by blue LED. The illumination time intervals (shown at the top of the graphs) were fixed at 5 min for the UV-LED and 10 min (a); or 8 min (b) for the blue LED. In both cases, the applied voltage was 100 V_{RMS} at a frequency of 1 kHz. The temperature of the film held at 26 °C. UV light intensity: 1.8 mW cm⁻² (a) and 5 mW cm⁻² (b).

The UV-light-produced change becomes like an enhancement of the film transparency. As such, the film transparency is increased within the whole range of AC voltage we have applied. An interesting maximum-shaped dependence on the AC voltage takes place for the ratio η_{UV} of the field-dependent transmittance of UV-light-illuminated ANPs/7CB/EPH film to the same behaviour but measured upon illumination with blue light (Fig. 9b). Since the degree of the UV-light induced effect (η_{UV}) can be electrically commanded by the field, this could be an attractive option for light-controllable electro-optics.

In fact, the effect from UV illumination is expressed as a large shift (in our case, by more than 25 V) of the curve of field-dependent transmittance of the ANPs/7CB/EPH films toward the lower voltages of the applied AC electric field. As such, this light-induced effect can be very useful from practical point of view. Both the increase of light transmittance of the films by increasing electric field above the distinct threshold, as well as the reduction of the threshold voltage for the light transmittance characteristics of EPH-doped ANPs/7CB upon UV light, were compatible with our optical microscopy observations. No such features were found for the corresponding characteristic curves obtained for the undoped ANPs/7CB nanocomposite films, being in identical cells under identical experimental conditions.

By switching-off the UV lightening followed by illumination with blue light whose spectral band is centered at 455 nm (see Fig. 4a) and overlaps the absorption of the EPH *cis*-form (the peak corresponding to $n - \pi^*$ band of the azobenzene group, close to 450 nm (e.g., [43]), Fig. 4b), the ANPs/7CB/EPH system reverts to its initial state and restores the initial transmittance curve (Fig. 9a). The recovery process can well be seen by switching the UV and blue lights alternatively (Fig. 10a). Since the spectrum of the blue LED used here explicitly activates the EPH dopants via the well known mechanism of *cis*-to-*trans* photoisomerization of azobenzene molecules (e.g., [43,44]), the above test evidences that just the component EPH and its photoisomerization are only responsible for the photoactive alteration of the electro-optics of the studied ANPs/7CB/EPH films. The light-controlled recovery of the EO response is an important application aspect.

The stability of the photo-switching by the studied ANPs/7CB/EPH nanocomposite films was probed by repeating cycles. To accelerate and intensify the *cis*-isomerization of EPH, we used in this test a higher exposure dose of the UV light. For example, Fig. 10(b) reports a switching cycle test of ANPs/7CB/EPH film being permanently upon AC electric field. The temporal series

was recorded upon illumination by repeating cycles of alternating switching (on/off) of the UV and blue lights, as shown in the graph. The test indicates that after few cycles of *trans*-*cis*-*trans* isomerization, the ANPs/7CB/EPH system does not hold the UV-activated photostationary state, i.e. the saturation regime that was completely reached during the UV illumination (Fig. 10b), and this state is not fully recovered. Taking into account the high thermo-physical stability of the azobenzene dopant, most probably, this is due to local heating caused by the UV light (as well as by the some accumulated heat during the subsequent illumination with blue light) that leads to thermal *cis*-to-*trans* isomerization, a process well known for azo compounds (the metastable *cis* state is thermally reconvert to the *trans*) (e.g., [45,46]). The kinetics of the thermal back reaction of azo compounds, azopolymers, azo-LCs and azo-doped LCs [23,47–49] strongly depends on the local heating, i.e. on the light fluence. The above test illustrates that such photo-induced thermal reaction of our nematic nanocomposites may limit their usage in applications that require good long-term stability of the photo-switching. The reversibility of the photo-switching of the studied azobenzene-LC-containing photoresponsive nanofilled nematic gels is not so sufficient as the photo-switching of azopolymers (amorphous or liquid-crystalline) or polymer-azobenzene complexes that have been shown to exhibit excellent long-term stability in photo-induced changes (e.g., [50,51]). Clearly, the sizable UV light absorption by the host ANPs/7CB gel itself (recall Fig. 3) strongly contributes to the local heating in our case. The time-stability test we have performed simply indicates that for a reversible photo-induced switching based on *trans*-*cis* photoisomerisation of azobenzene LC EPH and to achieve efficient photo-controllable electro-optics of ANPs/7CB/EPH nanocomposite films reported here, the dose of the UV light has to be carefully portioned.

3.2.2. EO modulation

The photoactive azo-bonded EPH molecules included in the ANPs/7CB nanocomposite films can modify also their amplitude-frequency EO modulation characteristics. Fig. 11 reports the frequency-dependent second-harmonic modulation of light passed through ANPs/7CB/EPH nanocomposite film, as recorded without or in the presence of UV illumination. As seen, the amplitude of second-harmonic EO modulation can be altered with UV light, in our case, a modulation enhancement by a factor up to 10 can be achieved (this UV-light-produced change is reduced by increasing magnitude of the applied AC electric field). Further, the slope of

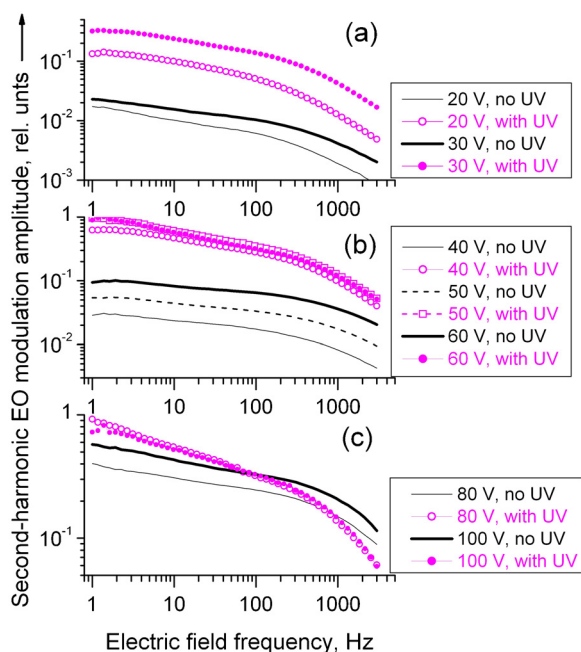


Fig. 11. UV-light produced effect on the EO second-harmonic modulation by EPH-doped ANPs/7CB film, as measured at various AC voltages (under identical other experimental conditions). He-Ne laser beam was employed as a probe light. The temperature of the film was 26 °C.

second-harmonic EO modulation spectrum can be also changed by UV lightening, an effect that is well pronounced at a stronger field (Fig. 11c). Like the AC voltage-dependent transmittance of the ANPs/7CB/EPH films (discussed in Section 3.2.1), with blue light one can perform the reverse *cis*-to-*trans* conformation of EPH molecules, and thereby, the recovery of the modulation behaviour that takes place in the non-illuminated case. Thus, the EO modulation by azo-doped nematic nanocomposite films studied here can be photo-controlled to some extent.

As reported in [16], the slope of the frequency spectra of the EO second-harmonic modulation by ANPs/7CB nanocomposite films is decreased by increased electric field and this slope is considerably smaller than that by the pure 7CB itself [16] (where contribute the large bulk LC domains). By this specific EO effect, the modulation spectra (EO response modulated by the dielectric oscillations of the nematic director) measured at the doubled frequency of the driving AC electric field, become rather flat and extended towards the higher frequencies of the field if the field strength is high enough. In the nanostructured nematic gel, the smaller the size of the active bulk domains, the smaller is the slope of the EO second-harmonic modulation spectra (e.g., over the frequency range 1–1000 Hz and at higher amplitude of the electric field [16]). The larger slopes of the EO second-harmonic frequency-modulation characteristics of ANPs/7CB/EPH nanofilled nematic system upon UV light (Fig. 11, especially Fig. 11b,c) suggest an enlargement of the dimensions of the local bulk domains in this system upon UV light (or related effect).

3.3. Explanation of the observed photo-stimulated EO effect in ANPs/7CB/EPH system

The UV-light induced lowering of the threshold voltage observed for the AC field-dependent optical transmittance of ANPs/7CB/EPH films (Fig. 9a) should be discussed in terms of local Fréedericksz transition in the considered nanofilled nematic [29] doped with photoisomerizable LC molecules, as modified by UV illumination (if there was no ANPs network, we should

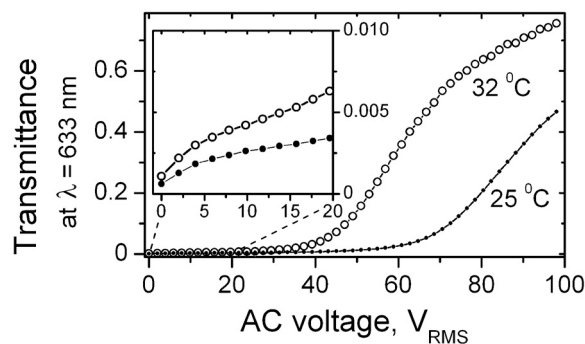


Fig. 12. Electric-field-dependent light transmittance of non-illuminated ANPs/7CB/EPH film at temperatures of 25 °C (open circles) and 32 °C (solid circles). The frequency of the electric field applied on the film was 1 kHz. The inset: the expanded low-voltage region of the same plots.

have a planar orientation of the film that provides developing of bulk Fréedericksz transition). For this, the anisotropic EPH-ANPs, ANPs-LC and EPH-LC surface and molecular interactions in the anisotropic environment of LC matrix should be also taken into account. Generally, in this case the corresponding EO mechanism of the UV-light induced lowering of the Fréedericksz voltage is rather complex and will be given in details elsewhere.

Phenomenologically, the observed photo-stimulated EO effect should be regarded as electrical quenching of static light scattering by nano-disordered nematic. Central point in the interpretation would then be the influence of various applied factors upon the electric coherence length (ξ) [52] of the distorted regions around the chains of ANPs. The reduction of ξ brings about a smoothing of refractive indices' gradients, and thus reduction of light scattering.

Upon UV illumination, the non-rod-like shaped (the *cis* form) azo molecules induce a shift of the nanostructured system toward the isotropic phase. This is consistent with the reduction of the order parameter (S) of the system that is normally expected because of anisometry reduction of the EPH LC molecules being in their *cis* forms. According to theory [52], ξ is going to decrease with temperature taking into account the dependence of S on the elastic and dielectric constants. This effect can be proven by the electrical quenching behaviour (the electric-field-dependent optical transmittance) of our ANPs/7CB/EPH films measured (in the absence of UV illumination) at two different temperatures within the range of the nematic phase of the ANPs/7CB/EPH system (Fig. 12). Like the threshold voltage shift of ~ 25 V seen in Fig. 9(a), a difference of ~ 25 V between these two characteristic curves (at their steepest slopes) is evident in Fig. 12 when the temperature differs by 7 °C. By UV illumination under identical conditions, nearly the same temperature shift (related to the depression of the clearing point by the UV light) is present in the temperature-dependent optical transmittance of the same film (Fig. 7). In this way we demonstrate that the mechanism behind the observed UV-light induced effect is associated with a decrease of S . Such interpretation also explains why an increase of the molecular disorder, i.e. reduction of ξ , under UV illumination leads to remarkable contribution to electrical quenching of light scattering, as observed (Fig. 9a). Reduction of the light scattering by the ANPs/7CB/EPH nematic system could be expected even without electric field applied, but upon UV illumination (as indeed registered – see the insets in Figs. 7 and 9a).

3.4. Light control of ANPs/7CB/EPH electro-optics (application aspect)

The photo-controllable scatter-based electro-optics by ANPs/7CB/EPH nematic nanocomposites discussed above is interesting from an application point of view. It should be empha-

sized that the large UV-light induced reducing of the threshold voltage of the voltage-dependent transmittance demonstrated for the presently studied photo-sensitized nanofilled nematic films (recall Fig. 9a), is quite unusual. It is achieved owing to the nanostructure imposed by the aerosil network within the nematic system and the LC confinement in the gel network. The observed large photo-stimulated lowering of the threshold voltage is not possible for a simple azo-doped nematic, e.g., EPH/7CB guest-ghost mixture, where such an effect is expected to be very small. For the sake of comparison, the Fréedericksz threshold of guest-host mixture of 3.4 wt.% EPH in 7CB in similar planar cells and in the nematic phase is equal to 2 V [42] (0.9 V for the nematic 7CB itself).

As seen from Fig. 9(b), the extent (η_{UV}) of the observed UV-light induced effect is rather strong. For the experimental data given in Fig. 9, η_{UV} was over 30, i.e. up to degree being of interest for practical application. Further, depending on the registration regime, η_{UV} can be considerably enlarged. The experimental data in Fig. 9 were obtained within a collection spatial angle of 0.6° . If the photodiode detector is placed at a larger distance from the sample, i.e. the light passed through the films is registered in the far-wave zone that corresponds to a reduced effect from diffuse light scattering from the films (at the wavelength of the probe laser beam used for the measurements) and at collection spatial angle reduced up to the divergence limit for the same collimated laser beam, then the maximum of η_{UV} can reach even 80–100 for the same ANPs/7CB/EPH sample (and at the same AC voltage ~ 60 V as in Fig. 9b).

In fact, at a given temperature corresponding to nematic phase of ANPs/7CB/EPH, over a relatively large AC voltage range this nanocomposite exhibits two stable and well differentiated photo-commanded states for its voltage-dependent optical transmittance: (i) an 'OFF' state, with a minimized transparency owing to maximum EPH *trans*-isomers (and minimum *cis*-isomers) produced and controlled with a blue light; and (ii) UV light-activated state with maximum *cis*-conformed EPH and enhanced light transmittance ('ON' state) (Figs. 9 and 10). Both EO states can be electrically- and photo-controlled. In a certain voltage range, a large dynamic range (contrast) between the values of the optical transmittance relevant to these states can be achieved, being useful feature of the proposed photoactive ANPs/7CB/EPH nanocomposites. We have to mention that such their function is in the frequency range generally considered to be the dielectric regime (kHz) of operation of LC devices. In the low-frequency range (<10 Hz) referred as the conducting regime when the ions in the LC medium influence its electrical properties, both UV-light induced shifts (of the phase transition temperature and the threshold voltage for EO operation, reported above) for the ANPs/7CB/EPH nematic system can be strongly diminished.

The observed photo-stimulated effect on the electro-optics of the studied ANPs/7CB/EPH films may be more useful if a larger and faster light-induced modification of their EO characteristics can be achieved, as well as a rapid recovery. This may be done by more intensive and quick photoisomerization of the EPH photoactive agent. The acceleration of the photoisomerization process might be performed with high-power optical pulses (e.g., from short-pulsed lasers), thereby enabling more efficient light control, or by applying a DC bias voltage [42]. Surely, the use of more intense light impact will enhance the considered photo-stimulated effect and will improve the performance of light-controllable EO devices based on such LC nanocomposites with *trans-cis* photoisomerizable agent. At best, an acceleration of the light control on the EO response can be implemented by lasers radiating UV/blue-light in short and ultra-short pulses (e.g., in the nano- to femto-second scales) (work in progress). Such light pulse duration ensures high-intensity optical field and in the same time by ultra-short pulses one can avoid the light-induced local thermo-effects due to the optical absorption, thereby preventing the non-desirable thermal

degradation of the photoresponsive nanocomposite organic material.

Finally, very important from an application's point of view is the long-term stability (as well the possible aging, unwanted) of the photoactive nematic nanocomposite proposed here. As relevant to potential applications, we have proved the photo-controlled EO response of this material in a time period of more than two years. The tests indicated that both the static and dynamic EO characteristics of the inspected optical films of EPH-doped ANPs/7CB nanocomposite remain the same when keeping the same experimental conditions, i.e., the produced nanocomposite material is photo- and thermo-stable, did not undergo any irreversible changes and its functionality has not been changed with time during this period.

4. Conclusions

We have composed a stable photoresponsive nanofilled nematic of 3 wt.% aerosil (silica nanospheres with a mean diameter of about 7 nm) and nematic 7CB as doped with photoactive azobenzene nematic (namely, EPH). Upon simultaneous application of AC electric field and by illuminating with appropriate UV light, thin films of such room-temperature nanostructured nematic exhibit modified EO properties. In particular, the inclusion of relatively small amount of 3 wt.% EPH into the nematic aerosil/7CB nanogel allows both the static (the AC electric-field-controlled transmittance) and the frequency-doubled EO modulation characteristics of thin films (25 μm) of the composed aerosil/7CB/EPH nanofilled nematic material to be efficiently changed by light.

The demonstrated photo-stimulated EO effect occurs owing to the nano(aerosil) network within the studied azo-doped nanofilled nematic. This effect is photo-driven by the facile light-induced steric effect of molecular conformation change of the azo-bonded molecules (the transformation of EPH from *trans* to *cis* isomers, and vice versa) within the illuminated area of thin films of this nanocomposite. Thereby, the EPH-doped nanofilled aerosil/7CB nematic provides a photo-activated ON-OFF switching through two distinct EO states that are photo- and electrically-controllable. The underlying cause for the observed photo-driven effects and light-modified EO behaviors of the aerosil/7CB/EPH nematic is the photo-induced change of magnitude of the nematic short range order.

The efficient light- and AC field-control makes the photoresponsive nano(aerosil)-filled nematic systems attractive for specific scatter-based room-temperature EO applications, such as photo-controllable EO switches and attenuators (working by transmitted light), in amplitude-frequency modulators, as well as for photonics and sensorics based on photo-sensitive electro-optics. Reasonably, of great importance for the engineering of such photoactive nanocomposites are the concentrations of both nanoscale dopants - the aerosil nanoparticles and the azo-bonded molecules. Besides the suitable concentration of the photosensitizer, for sufficient light-induced stimulation of the electro-optics of these materials one has to consider also the illuminating light intensity, as well as the amplitude of the applied AC electric field. Furthermore, the size of the effect reported here strongly depends on the temperature.

Conflicts of interest

There is no conflict of interest. The authors have no other relevant affiliations or financial involvement with any organization or entity with a financial interest in or financial conflict with the subject matter or materials discussed in the manuscript. This includes employment, consultancies, stock ownership or options, expert testimony, grants or patents received or pending, or royalties.

Acknowledgements

The authors acknowledge the financial support by the Ministry of Education and Science, National Science Fund of Bulgaria, as well as by the Department of Science and Technology, Ministry of Science and Technology, New Delhi, India, under Indo-Bulgarian joint research project DNTS/In-01/4/2013. A part of this study was carried out in the frame of the research project DFNI-TO2/10 by the Ministry of Education and Science, National Science Fund of Bulgaria.

References

- [1] H. Stark, Physics of colloidal dispersions in nematic liquid crystals, *Phys. Rep.* 351 (2001) 387–474, [http://dx.doi.org/10.1016/S0370-1573\(00\)00144-7](http://dx.doi.org/10.1016/S0370-1573(00)00144-7).
- [2] Y.A. Garbovskiy, A.V. Glushchenko, Liquid crystalline colloids of nanoparticles: preparation, properties and applications, in: R.E. Camley, R.L. Stamps (Eds.), *Solid State Physics*, vol. 62, Academic Press, Elsevier, San Diego, CA, USA, 2011, pp. 1–74.
- [3] J.P.F. Lagerwall, G. Scalia, A new era for liquid crystal research: applications of liquid crystals in soft matter nano-, bio- and microtechnology, *Curr. Appl. Phys.* 12 (2012) 1387–1412, <http://dx.doi.org/10.1016/j.cap.2012.03.019>.
- [4] C. Blanc, D. Coursault, E. Lacaze, Ordering nano- and microparticles assemblies with liquid crystals, *Liq. Cryst. Rev.* 1 (2013) 83–109, <http://dx.doi.org/10.1080/21680396.2013.818515>.
- [5] A. Hauser, O.V. Yaroshchuk, H. Kresse, Aerosil in liquid crystals, *Mol. Cryst. Liq. Cryst. Sci. Technol. Section A. Mol. Cryst. Liq. Cryst.* 330 (1999) 407–414, <http://dx.doi.org/10.1080/10587259908025616>.
- [6] T. Kato, Self-assembly of phase-segregated liquid crystal structures, *Science* 295 (2002) 2414–2418, <http://dx.doi.org/10.1126/science.1070967-a>.
- [7] G.S. Iannacchione, Review of liquid-crystal phase transitions with quenched random disorder, *Fluid Phase Equilibria* 222–223 (2004) 177–187, <http://dx.doi.org/10.1016/j.fluid.2004.06.022>.
- [8] S.K. Prasad, K.L. Sandhya, G.G. Nair, U.S. Hiremath, C.V. Yelamaggad, S. Sampath, Electrical conductivity and dielectric constant measurements of liquid crystal-gold nanoparticle composites, *Liq. Cryst. Sci. Technol.* 33 (2006) 1121–1125, <http://dx.doi.org/10.1080/02678290600930980>.
- [9] M. Marinelli, A.K. Ghosh, F. Mercuri, Small quartz silica spheres induced disorder in octylcyanobiphenyl (8CB) liquid crystals: a thermal study, *Phys. Rev. E* 63 (1–9) (2001), 061713, <http://dx.doi.org/10.1103/PhysRevE.63.061713>.
- [10] A. Rosh, G.S. Iannacchione, P.S. Clegg, R.J. Birgeneau, Evolution of the isotropic-to-nematic phase transition in octyloxycyanobiphenyl+aerosil dispersions, *Phys. Rev. E* 69 (1–11) (2004) 031703, <http://dx.doi.org/10.1103/PhysRevE.69.031703>.
- [11] C.V. Lobo, S.K. Prasad, C.V. Yelamaggad, Experimental investigations on weakly polar liquid crystal-aerosil composites, *J. Phys.: Condens. Matter* 18 (2006) 767–776, <http://dx.doi.org/10.1088/0953-8984/18/3/002>.
- [12] V. Jayalakshmi, G.G. Nair, S.K. Prasad, Effect of aerosil dispersions on the photoinduced nematic-isotropic transition, *J. Phys.: Condens. Matter* 19 (226213) (2007) 1–12, <http://dx.doi.org/10.1088/0953-8984/19/22/226213>.
- [13] M. Kreuzer, R. Eidenschink, Filled nematics, in: G.P. Crawford, S. Zumer (Eds.), *Liquid Crystals in Complex Geometries Formed by Polymer and Porous Networks*, Taylor & Francis, London, UK, 1996, pp. 307–324.
- [14] C.Y. Huang, C.C. Lai, Y.H. Tseng, Y.T. Yang, C.J. Tien, K.Y. Lo, Silica-nanoparticle-doped nematic display with multistable and dynamic modes, *Appl. Phys. Lett.* 92 (1–3) (2008), <http://dx.doi.org/10.1063/1.2938880>, 221908.
- [15] C.Y. Huang, Y.J. Huang, Y.H. Tseng, Dual-operation-mode liquid crystal lens, *Opt. Express* 17 (2009) 20860–20865, <http://dx.doi.org/10.1364/OE.17.020860>.
- [16] Y.G. Marinov, G.B. Hadjichristov, A.G. Petrov, S.K. Prasad, Electro-optic modulation by silica-nanostructured nematic system (aerosil/7CB nanocomposite, *Compos. Part B-Eng.* 90 (2016) 471–477, <http://dx.doi.org/10.1016/j.compositesb.2016.01.034>.
- [17] Y.G. Marinov, G.B. Hadjichristov, A.G. Petrov, S. Krishna Prasad, Thin films of silica nanoparticle doped nematic liquid crystal 7CB for electro-optic modulation, *Photon. Lett. Pol.* 7 (2015) 94–96, <http://dx.doi.org/10.4302/plp.2015.4.03>.
- [18] S.K. Prasad, G.G. Nair, G. Hegde, K.L. Sandhya, D.S.S. Rao, C.V. Lobo, C.V. Yelamaggad, Photoinduced effects in nematic liquid crystals, *Phase Transit.* 78 (2005) 443–455, <http://dx.doi.org/10.1080/01411590500185690>.
- [19] A.G. Petrov, Y.G. Marinov, G.B. Hadjichristov, S. Sridevi, U.S. Hiremath, C.V. Yelamaggad, S.K. Prasad, New photoactive guest-host nematics showing photoflexoelectricity, *Mol. Cryst. Liq. Cryst.* 544 (2011) 3/[991]–13/[1001], <http://dx.doi.org/10.1080/15421406.2011.569221>.
- [20] S. Sridevi, U.S. Hiremath, C.V. Yelamaggad, S.K. Prasad, Y.G. Marinov, G.B. Hadjichristov, A.G. Petrov, Behaviour of photosensitive soft materials: thermo-optical, dielectric and elastic constant studies on azo-dye doped nematic liquid crystals, *Mater. Chem. Phys.* 130 (2011) 1329–1335, <http://dx.doi.org/10.1016/j.matchemphys.2011.09.027>.
- [21] C.V. Yelamaggad, S.K. Prasad, Q. Li, Photo-stimulated phase transformations in liquid crystals and their non-display applications, in: Q. Li (Ed.), *Liquid Crystals Beyond Displays*, Chemistry, Physics, and Applications, John Wiley & Sons, Hoboken, NJ, USA, 2012, pp. 155–211.
- [22] J. Mysliwiec, A. Miniewicz, S. Nespurek, M. Studenovskiy, Z. Sedlakova, Efficient holographic recording in novel azo-containing polymer, *Opt. Mater.* 29 (2007) 1756–1762, <http://dx.doi.org/10.1016/j.optmat.2006.10.003>.
- [23] A. Miniewicz, H. Orlikowska, A. Sobolewska, S. Bartkiewicz, Kinetics of thermal cis–trans isomerization in a phototropic azobenzene-based single-component liquid crystal in its nematic and isotropic phases, *Phys. Chem. Chem. Phys.* 20 (2018) 2904–2913, <http://dx.doi.org/10.1039/C7CP06820D>.
- [24] E. Schab-Balcerzak, A. Sobolewska, A. Miniewicz, J. Jurusik, Chromophore concentration effect on holographic grating formation efficiency in novel azobenzene-functionalized polymers, *Polym. Eng. Sci.* 48 (2008) 1755–1767, <http://dx.doi.org/10.1002/pen.21140>.
- [25] A. Miniewicz, J. Mysliwiec, F. Kajzar, J. Parka, On the real-time reconstruction of digital holograms displayed on photosensitive liquid crystal systems, *Opt. Mater.* 28 (2006) 1389–1397, <http://dx.doi.org/10.1016/j.optmat.2005.08.020>.
- [26] Y.G. Marinov, G.B. Hadjichristov, A.G. Petrov, S.K. Prasad, Photo-controllable electro-optics of aerosil/7CB nanocomposite nematic doped with azo-bonded molecules, *J. Phys.: Conf. Ser.* 682 (1–5) (2016) 012030, <http://dx.doi.org/10.1088/1742-6596/682/1/012030>.
- [27] G.B. Hadjichristov, Y.G. Marinov, Photoresponsive azo-doped aerosil/7CB nematic liquid-crystalline nanocomposite films: the role of polyimide alignment layers of the films, *J. Phys.: Conf. Ser.* 780 (1–7) (2017) 012008, <http://dx.doi.org/10.1088/1742-6596/780/1/012008>.
- [28] Y.G. Marinov, G.B. Hadjichristov, A.G. Petrov, S.K. Prasad, Photoresponsive azo-doped aerosil/7CB nematic nanocomposites: the effect from concentration of the azobenzene photoactive agent, *J. Phys.: Conf. Ser.* 794 (1–7) (2017) 012037, <http://dx.doi.org/10.1088/1742-6596/794/1/012037>.
- [29] M.V. Kumar, S.K. Prasad, Y. Marinov, L. Todorova, A.G. Petrov, Flexo-dielectric-optical spectroscopy as a method of studying nanostructured nematic liquid crystals, *Mol. Cryst. Liq. Cryst.* 610 (2015) 51–62, <http://dx.doi.org/10.1080/15421406.2015.1025205>.
- [30] B.R. Ratna, R. Shashidhar, Dielectric properties of 4'-n-alkyl-4-cyanobiphenyls in their nematic phases, *Pramana* 6 (1976) 278–283 http://www-old.ias.ac.in/j_archive/pramana/6/5/278-283/viewpage.html.
- [31] G.S. Iannacchione, C.W. Garland, J.T. Mang, T.P. Rieker, Calorimetric and small angle x-ray scattering study of phase transitions in octylcyanobiphenyl-aerosil dispersions, *Phys. Rev. E* 58 (1998) 5966–5981, <http://dx.doi.org/10.1103/PhysRevE.58.5966>.
- [32] R. Bandyopadhyay, D. Liang, R.H. Colby, J.L. Harden, R.L. Leheny, Enhanced elasticity and soft glassy rheology of a smectic in a random porous environment, *Phys. Rev. Lett.* 94 (1–4) (2005), 107801, <http://dx.doi.org/10.1103/PhysRevLett.94.107801>.
- [33] Y.G. Marinov, G.B. Hadjichristov, A.G. Petrov, S. Sridevi, U.S. Hiremath, C.V. Yelamaggad, S.K. Prasad, Trans-cis photoisomerization-induced tilted anchoring in photoactive guest-host liquid crystalline systems, *J. Phys. Conf. Ser.* 398 (1–6) (2012) 012038, <http://dx.doi.org/10.1088/1742-6596/398/1/012038>.
- [34] M. Mizuno, T. Shinoda, H. Mada, S. Kobayashi, Electronic spectra of 4-n-heptyl-4'-cyanobiphenyl (7CB) in nematic and isotropic liquid states, *Mol. Cryst. Liq. Cryst.* 56 (1979) 111–114, <http://dx.doi.org/10.1080/01406567908071977>.
- [35] J. Cooper, Compositional analysis of Merck E7 liquid crystal intermediates using ultra performance convergence chromatography (UPC2) with PDA detection, in: Application Note–Merck Liquid Crystal Custom Report, Waters Corporation, Manchester, UK, 2013, pp. 1–7; <http://www.waters.com/webassets/cms/library/docs/720004814en.pdf>, (Accessed 11 October 2017).
- [36] S. Lee, C. Park, Agglomeration of silica nanoparticles in filled nematic liquid crystals, *Mol. Cryst. Liq. Cryst.* 333 (1999) 123–134, <http://dx.doi.org/10.1080/10587259908025999>.
- [37] S.B. Lee, K. Nakayama, T. Matsui, M. Ozaki, K. Yoshino, Structure and dynamics in liquid crystals of suspensions of silica particles under a low frequency AC applied voltage, *IEEE Trans. Dielectr. Electr. Insul.* 9 (2002) 31–38, <http://dx.doi.org/10.1109/94.983881>.
- [38] T. Bellini, N.A. Clark, Light scattering as a probe of liquid crystal ordering in silica aerogels, in: G.P. Crawford, S. Zumer (Eds.), *Liquid Crystals in Complex Geometries Formed by Polymer and Porous Networks*, Taylor & Francis, London, UK, 1996, pp. 381–410.
- [39] F. Mercuri, A.K. Ghosh, M. Marinelli, Disorder effects in low concentration dispersions of small quartz spheres in cyanobiphenyl liquid crystals, *Phys. Rev. E* 60 (1999) R6309–R6312, <http://dx.doi.org/10.1103/PhysRevE.60.R6309>.
- [40] T. Bellini, M. Buscaglia, C. Chiccoli, F. Mantegazza, P. Pasini, C. Zannoni, Nematics with quenched disorder: what is left when long range order is disrupted? *Phys. Rev. Lett.* 85 (2000) 1008–1011, <http://dx.doi.org/10.1103/PhysRevLett.85.1008>.
- [41] M. Caggioni, A. Rosh, S. Barjani, F. Mantegazza, G.S. Iannacchione, T. Bellini, Isotropic to nematic transition of aerosil-disordered liquid crystals, *Phys. Rev. Lett.* 93 (1–4) (2004), 127801, <http://dx.doi.org/10.1103/PhysRevLett.93.127801>.
- [42] S.K. Prasad, G.G. Nair, V. Jayalakshmi, Electric-field-assisted acceleration of the photostimulated nematic-isotropic transition, *Adv. Mater.* 20 (2008) 1363–1367, <http://dx.doi.org/10.1002/adma.200701393>.

- [43] Y. Zhao, T. Ikeda (Eds.), *Smart Light-Responsive Materials: Azobenzene-Containing Polymers and Liquid Crystals*, John Wiley & Sons, Hoboken, NJ, 2009.
- [44] K.G. Yager, C.J. Barrett, Novel photo-switching using azobenzene functional materials, *J. Photochem. Photobiol. A* 182 (2006) 250–261, <http://dx.doi.org/10.1016/j.jphotochem.2006.04.021>.
- [45] N. Böhm, A. Materny, W. Kiefer, H. Steins, M.M. Müller, G. Schottner, Spectroscopic investigation of the thermal cis-trans isomerization of disperse red 1 in hybrid polymers, *Macromolecule* 29 (1996) 2599–2604, <http://dx.doi.org/10.1021/ma951238o>.
- [46] D.G. Whitten, P.D. Wildes, J.G. Pacifici, G. Irick Jr., Solvent and substituent effects on the thermal isomerization of substituted azobenzenes. A flash spectroscopic study, *J. Am. Chem. Soc.* 93 (1971) 2004–2008, <http://dx.doi.org/10.1021/ja00737a027>.
- [47] J. Garcia-Amorós, A. Sánchez-Ferrer, W.A. Massad, S. Nonell, D. Velasco, Kinetic study of the fast thermal cis-to-trans isomerisation of para-, ortho- and polyhydroxyazobenzenes, *Phys. Chem. Chem. Phys.* 12 (2010) 13238–13242, <http://dx.doi.org/10.1039/c004340k>.
- [48] J. Garcia-Amoros, H. Finkelmann, D. Velasco, Role of the local order on the thermal cis-to-trans isomerisation kinetics of azo-dyes in nematic liquid crystals, *Phys. Chem. Chem. Phys.* 13 (2011) 11233–11238, <http://dx.doi.org/10.1039/C1CP20280D>.
- [49] J. Garcia-Amoros, D. Velasco, Understanding the fast thermal isomerisation of azophenols in glassy and liquid-crystalline polymers, *Phys. Chem. Chem. Phys.* 16 (2014) 3108–3114, <http://dx.doi.org/10.1039/C3CP54519A>.
- [50] M.V. Srinivasan, P. Kannan, Photo-switching and nonlinear optical behaviors of center linked bent-core azobenzene liquid crystalline polymers, *J. Mater. Sci.* 46 (2011) 5029–5043, <http://dx.doi.org/10.1007/s10853-011-5423-x>.
- [51] J. Vapaavuori, C.G. Bazuin, A. Priimagi, Supramolecular design principles for efficient photoresponsive polymer-azobenzene complexes, *J. Mater. Chem. C* 6 (2018) 2168–2188, <http://dx.doi.org/10.1039/c7tc05005d>.
- [52] P.G. de Gennes, J. Prost, *The Physics of Liquid Crystals*, second edition, Clarendon Press - Oxford/ Oxford University Press, New York, USA, 1993, pp. 108–123.